Generic Magnetic Fusion Rocket Model

J.F. Santarius and B.G. Logan

April 1993
(revised February 1998)

UWFDM-914

Prepared for the 29th AIAA/SAE/ASME/ASEE Joint Propulsion Conference, Paper AIAA-93-2029, June 28–30, 1993, Monterey CA.

FUSION TECHNOLOGY INSTITUTE

UNIVERSITY OF WISCONSIN

MADISON WISCONSIN

Generic Magnetic Fusion Rocket Model

J.F. Santarius and B.G. Logan

Fusion Technology Institute
University of Wisconsin
1500 Engineering Drive
Madison, WI 53706

http://fti.neep.wisc.edu

April 1993 (revised February 1998)

UWFDM-914

Prepared for the 29th AIAA/SAE/ASME/ASEE Joint Propulsion Conference, Paper AIAA-93-2029, June 28–30, 1993, Monterey CA.

Generic Magnetic Fusion Rocket Model

John F. Santarius*

University of Wisconsin, Madison, Wisconsin 53706

and

B. Grant Logan†

Lawrence Livermore National Laboratory, Livermore, California 94550

A generic magnetic fusion rocket model is developed and used to explore the limits of magnetic fusion propulsion systems. Two fusion fuels are examined, D-T and D-^{3}He, and the D-^{3}He fuel cycle is predicted to give a higher specific power for optimized parameters. Other findings are that (1) magnetic fusion should ultimately be able to deliver specific powers of ~ 10 kW/kg and (2) specific powers of 1–5 kW/kg should be achievable with only modest extrapolations of present technology.

Presented as Paper 93-2029 at the AIAA/SAE/ASME/ASEE 29th Joint Propulsion Conference, Monterey, CA, June 28–30, 1993.

*Senior Scientist, Fusion Technology Institute, 1500 Engineering Drive. Member AIAA

†Associate Program Leader, Inertial-Confinement Fusion Applications, P.O. Box 808, Mail Stop L-481.

Nomenclature

B = magnetic field

C_m = magnet structure design safety factor

D = deuterium

E = energy per reaction

E_{stored} = magnet stored energy

f_{burn} = tritium burn fraction

^3He = helium-3

^4He = helium-4

M_m = Magnet mass

n = density

n = neutron

p = proton

P = power

Q = fusion power/input power

r_w = wall radius

T = plasma temperature

T = tritium

V_{mag} = volume enclosed by magnetic field

α = specific power

β = plasma pressure/magnetic-field pressure

Δ_s = shield thickness

λ_s = shield thickness for ten-fold reduction of neutron power

μ_0 = magnetic permeability of free space

$\rho_{structure}$ = density of magnet structure

σ_{stress} = allowable magnet structure stress

$\langle \sigma v \rangle$ = Maxwellian-averaged fusion reaction rate

Subscripts

b = bremsstrahlung

ddn = D-D reaction neutron channel

ddp = D-D reaction proton channel

e = electron

f = fusion

i = ion

n = neutron

t = tritium

3 = helium-3

I. Introduction

The promise of magnetic fusion power for space propulsion throughout the Solar System was recognized in the late 1950's [1, 2, 3]. Since that time, fusion research has made great progress in experimental parameters, theoretical understanding, and the development of computer modeling tools. These advances have been used in several recent fusion space-propulsion conceptual design studies, listed in Table 1, which have predicted specific power values of α=1–10 $kW_{thrust}/kg_{reactor}$.

This paper describes a generic model of a magnetic fusion reactor for space propulsion. This model has been developed to examine the plausibility of the high specific powers that recent, more detailed studies have projected for fusion propulsion and to explore the limits on the performance that rockets powered by magnetic fusion might eventually achieve. The paper focusses on magnetic fusion energy, but it should be noted that work also exists on fusion using inertial confinement [4, 5] and electrostatic confinement [6, 7]. Several fusion propulsion options are compared in ref. [8], which attempted to evaluate the varying depth of detail of the existing studies in assessing them.

First, fusion fuels for space applications are discussed, followed by the equations used to model the physics and engineering systems. The results of parametric analyses are then presented and some optimized cases exhibited. Finally, conclusions are drawn. SI units are used, except that energies and temperatures are in keV.

II. Space Fusion Fuels

The two fusion fuel cycles expected to be most important for space propulsion applications are the reactions of deuterium and helium-3 and of deuterium and tritium:

$$\mathrm{D}+{}^3\mathrm{He} \rightarrow \mathrm{p}\ (14.68\ \mathrm{MeV})+{}^4\mathrm{He}\ (3.67\ \mathrm{MeV})$$

$$\mathrm{D}+\mathrm{T} \rightarrow \mathrm{n}\ (14.07\ \mathrm{MeV})+{}^4\mathrm{He}\ (3.52\ \mathrm{MeV})$$

The deuterium also increases the fusion power and the neutron production through the reactions:

$$\mathrm{D}+\mathrm{D} \rightarrow \mathrm{n}\ (2.45\ \mathrm{MeV})+{}^3\mathrm{He}\ (0.82\ \mathrm{MeV})$$

$$\mathrm{D}+\mathrm{D} \rightarrow \mathrm{p}\ (3.02\ \mathrm{MeV})+\mathrm{T}\ (1.01\ \mathrm{MeV})$$

Burnup of the tritium produced in the p+T channel contributes significantly to the neutron production for D-^{3}He fuel.

Several factors differentiate these fuel cycles. The main benefit of D-T fuel is that the fusion power density in the plasma can be much higher than for D-^{3}He, as shown in Fig. 2, and this makes the required *physics* parameters easier to achieve. D-^{3}He fuel, however, produces almost all of its fusion energy as charged particles, as shown in Fig. 3, and this results in several *engineering* advantages:

- Savings on the mass of the shield for the magnet and other components,
- The possibility for direct conversion of fusion power to thrust by guiding charged particles along magnetic-field lines,
- Higher availability and longer component lifetimes due to reduced radiation damage,
- Enhanced safety due to a lower radioactive inventory, and
- The elimination of a complex tritium-breeding blanket and processing system.

The last bullet assumes that tritium fuel would be bred on-board a D-T fusion rocket. Otherwise, 100 kg or more of radioactive tritium would need to be bred in another power plant, transported to the D-T fusion rocket, and carried in storage, with resulting safety and environmental concerns.

The availability of ^{3}He is also an issue, because ^{3}He is very rare on Earth. The ^{3}He resource problem has been solved, in principle, by the identification of a large amount of ^{3}He on the surface of the Moon [15, 16]. On the time frame of humankind's expansion into the Solar System, accessing the lunar ^{3}He resource appears to be well within technological capabilities [15, 16]. On an even longer time scale, the huge ^{3}He reserves of the Jovian planets should be within reach of human ingenuity. Suitable designs for breeding ^{3}He in D-D or other fusion reactors have been sought for over twenty years, and this work is summarized in ref. [17]. Although its feasibility appears doubtful, breeding may eventually provide a ^{3}He resource option. For D-^{3}He fusion research and development purposes, fortunately, a sufficient ^{3}He resource does exist on Earth [15, 16].

III. Description of the Model

A large variety of candidate magnetic fusion reactor configurations exists, with greatly differing geometries and plasma parameters. The present study assumes that the configuration of the external magnetic field coils is cylindrical—the choice of most of the detailed conceptual design studies for space propulsion [18]. Toroidal systems can be modeled approximately by equating the circumference of the major axis of the torus to the length of this cylinder. Compared to a toroidal configuration, the open-ended cylindrical geometry facilitates using the plasma for direct thrust and raises the ratio of the magnetic field in the plasma to the field on the coils. The basic geometry is shown in Fig. 1; it is particularly appropriate to configurations such as tandem mirrors, field-reversed configurations, and spheromaks [9, 19, 18, 20]. Although this model is very simple, the major components contributing to the total propulsion system mass—the magnets, shields, radiators, and refrigerators—are included and their masses can be estimated with reasonable accuracy.

The most important omission in this generic approach is the neglect of the mass of systems for input power and power conversion—which will vary significantly for differing configurations. Because the input power will typically be 10–100 MW to compensate for plasma transport and radiation losses, there will be a lower limit on the fusion power for a high-performance system due to the recirculating power. Therefore, the propulsion system thrust level chosen for the reference cases is 600 MW. For a nominal input power of 60 MW, this gives $Q = 10$, which is an approximate lower bound for the mass of the recirculating power system to be less than 10% of the total mass. This estimate is based on a conceptual design for direct conversion and power conditioning system masses in space [21, 22] plus the fact that neither radio-frequency (RF) antennas nor neutral beam injectors without their vacuum enclosures would have large masses.

Plasma physics

A useful characterization of magnetic fusion configurations is by the ratio of the plasma pressure to the magnetic field pressure,

$$\beta \equiv \frac{(n_e + n_i)T}{B^2/2\mu_0}. \tag{1}$$

Typical fusion-reactor β values range from 0.02–0.1 for the tokamak configuration to ~ 0.9 for the field-reversed configuration (FRC). These values depend on detailed calculations of magnetohydrodynamic (MHD) equilibrium and stability. Impurities and fusion 'ash' are neglected here, and equal ion and electron temperatures are assumed; these assumptions lead to relatively small corrections. The plasma density and temperature are assumed to have flat radial profiles, which is approximately true of many, but not all, of the types of configurations under consideration. Radially peaked values would necessitate an increase in the plasma radius. A 'halo' or 'scrape-off layer' of low-temperature plasma separates the core plasma from the chamber wall. This gap is taken to be 0.1 m for the present calculations to keep fusion products from hitting the wall due to their large gyroradii when they are born near the plasma edge with a high velocity perpendicular to the magnetic field.

The calculation of the total fusion power and the neutron power is straightforward, but it is complicated slightly in the D-^{3}He case by the need to include D-D reactions and the burnup of the tritium produced. The fraction of tritium burned up before it can escape the core plasma is assumed here to be 50%, a typical value [23] based on the particle confinement time being nearly equal to the energy confinement time. The D-^{3}He equations will be given explicitly; the D-T equations are analogous. The power terms are

$$\begin{aligned} P_f &= n_d n_3 \langle \sigma v \rangle_{d3} E_f^{d3} + \frac{n_d^2}{2} \langle \sigma v \rangle_{ddn} E_f^{ddn} + \frac{n_d^2}{2} \langle \sigma v \rangle_{ddp} E_f^{ddp} \\ &+ f_{burn} n_d n_t \langle \sigma v \rangle_{dt} E_f^{dt} \end{aligned} \tag{2}$$

$$P_n = \frac{n_d^2}{2} \langle \sigma v \rangle_{ddn} E_n^{ddn} + f_{burn} n_d n_t \langle \sigma v \rangle_{dt} E_n^{dt} \tag{3}$$

$$\begin{aligned} P_b &= 5.4 \times 10^{-43} n_e^2 T^{1/2} [0.00414 T + 0.070 Z_c^{eff} / T^{1/2} \\ &+ Z^{eff} (1 + 0.00155 T + 7.15 \times 10^{-6} T^2)] \end{aligned} \tag{4}$$

where it is important to include relativistic effects in the bremsstrahlung power [24], $Z^{eff} = \sum n_i Z_i^2 / n_e$, $Z_c^{eff} = \sum n_i Z_i^3 / n_e$, and the fusion reaction rate is given in ref. [25].

Synchrotron radiation power will also be generated, and it causes an unfavorable, but small, correction for the high betas and relatively low magnetic fields of most interest for space propulsion. The synchrotron power will be neglected for the present analysis. The power density for the remaining power loss from the core plasma, charged-particle transport, can be calculated by subtracting the neutron and bremsstrahlung powers from the sum of the fusion power and the input power. It is important to note, however, that the very difficult problem of the self-consistency of this transport power with the plasma dimensions and other parameters cannot be handled by a generic model, and transport sets a lower limit on the plasma radius. The transport power is available for generating thrust through the magnetic nozzle. These have received limited attention [26, 27], so it is unclear how high a thrust-to-transport power ratio (magnetic nozzle efficiency) will be attainable, and a reasonable value of 0.8 will be used here. The heat that must be rejected by the radiators will be the sum of the neutron and bremsstrahlung powers.

Engineering systems

The total magnet mass is taken to be the larger of two estimates, based on either the 'magnet virial theorem' or the winding-pack current density. The magnet virial theorem is related to the magnet structural mass limits due to material properties, and is given by

$$M_m = C_m \frac{\rho_{structure}}{\sigma_{stress}} E_{stored}. \tag{5}$$

where $C_m = 2$, $\rho_{structure} \simeq 2.5$ Mg/m^3 for carbon/carbon-composite structure), σ_{stress} is assumed to be 1000 MPa, and E_{stored} is given by

$$E_{stored} \simeq \frac{B^2}{2\mu_0} V_{mag} \tag{6}$$

The limit on the current density averaged over the magnet winding pack will be taken to range from 50 MA/m^2, typical of advanced fusion magnet conceptual designs and scheduled to be demonstrated on the Large Helical Device (LHD) fusion experiment in 1998 [28], to 250 MA/m^2, where superconductor quenching becomes a concern.

Assuming that conventional, low-temperature superconducting magnets are used and cooled by helium at 4.2 K, the mass of the helium refrigerators can be large. A value of 1000 kg/kW for the refrigerator mass per unit of heat deposited in the magnets is used here, which is $\sim$ 10 times better than present terrestrial helium refrigerators [29], because we have assumed improved technology, low mass as a design goal, and benefits from the low background temperature of space. Continued progress in *high-temperature* (>20 K) superconductors at the present pace for magnetic fields and current densities [30] would substantially improve fusion-propulsion performance by allowing higher refrigerator efficiency and radiation heating of magnets, thus reducing the mass of refrigerators, radiation shields, and magnets.

A shield is necessary to reduce the neutron flux from the plasma core to levels that protect the magnets from radiation damage and localized heating that could induce quenches. An optimized lithium hydride shield is used here [31], with a density of about 1 Mg/m^3. The neutron power absorbed in the magnet is

$$P_{mag} = P_n \left(\frac{r_w}{r_w + \Delta_s} \right) 10^{-\Delta_s/\lambda_s} \tag{7}$$

where the shield thickness required to reduce the neutron power by a factor of 10 is 0.31 m, and $r_w/(r_w + \Delta_s)$ is the geometric falloff of a line source with radius. The slight difference between the D-T and D-^{3}He neutron energy spectra is neglected. This assumption is conservative, especially at high ^{3}He-to-D density ratios, where a larger fraction of the neutron power is in the form of lower-energy, less-penetrating D-D neutrons. A space of 0.1 m is included between the shield and the magnet to account for thermal insulation, maintenance gaps, and support structure.

IV. Results

One purpose of the present study is to examine the likely performance of those fusion space propulsion systems which may, with a reasonably well-funded development program, be ready for use early in the twenty-first century. Another goal is to examine the ultimate limits of magnetic fusion for space propulsion. Thus, we focus upon two cases: (1) *Mid-term*: a modest extrapolation of present technology and (2) *Long-term*: an advanced case. The corresponding default assumptions are listed in Table 2.

To solve the equations presented in Sec. III, choices are made for β and the magnetic field. The specific power is then minimized over the variables shield thickness, plasma temperature, and ^{3}He-to-D density ratio, while varying the plasma length to give the desired thrust power and the plasma radius to satisfy either the heat flux limit in the D-^{3}He case or the neutron wall load limit in the D-T case. The D-T and D-^{3}He limiting effects differ because of the varying power distributions between neutrons and surface heat: respectively about 4:1 for D-T and 1:20 to 1:100 for D-^{3}He. For very short trips (approximately three months or less), the surface heat flux in a D-T reactor would reach its limit before the neutron wall load reached a sufficient fluence to exceed the damage limits for the structural materials. For uncrewed cargo missions, where a high payload fraction is more important than speed, or for travel to the outer Solar System, the trip would require at least six months and neutron damage would dominate. Several iterations are performed until the parameters vary by no more than a few percent, and these values are used to calculate the remaining quantities of interest.

Table 3 shows parameters for mid-term D-T and D-^{3}He cases and for a long-term D-^{3}He case. The calculations were performed using Mathematica^{TM} on a NeXT^{TM} computer. The mid-term D-T case shows the difficulty of achieving high specific power for this fuel cycle in a direct-thrust mode. The neutron wall load limit was set by the requirement that the structures experiencing the most radiation damage would last at least the lifetime of the mission. This is, of course, mission dependent, but even at high specific powers of $\alpha \simeq 10$ kW/kg, the shortest one-way Earth-Mars travel times are one month for payload fractions over 0.1 [32, 18], and these still favor D-^{3}He fuel.

The performance of D-T fuel will rise somewhat if more durable materials are developed, but dramatically improved performance appears unlikely. An interesting point for this case is that the superconducting magnets optimized at a field of 5 T due to the neutron wall load constraint on the system, not intrinsic limits of the superconductors themselves. Rather than using only the transport power for direct thrust, if the thermal D-T fusion power is converted to electricity and used to power a plasma thruster, the system may have some safety and environmental advantages over fission systems. The thermal conversion system will add a large mass, however, and the power density for a D-T reactor is expected to be near that of a fission reactor. It appears unlikely that specific powers significantly higher than the ~ 0.1 kW/kg expected of advanced fission systems will be reached.

The mid-term D-^{3}He case would provide an attractive specific power of ~ 5 kW/kg, suitable for greatly shortening trip times or increasing payload fractions compared to chemical or fission systems for travel throughout the Solar System [32, 33, 18]. The main extrapolation required is in the physics parameters, especially for the linear, cylindrically symmetric fusion configurations, which presently have only a limited data base. The projected performance is typical of earlier, more detailed studies of D-^{3}He fusion space propulsion systems, and shows why D-^{3}He fuel has usually been chosen over D-T fuel for space applications. The magnetic field optimized at 10 T in this case, representing a trade-off between higher plasma power density, which scales as B^4, and the surface heat flux limitation.

The long-term D-^{3}He case, at $\sim$ 10 kW/kg, is very attractive, although several of the engineering systems would require substantial development. The 12-T magnetic field is well below technological limits, as in the mid-term cases. This case has reached the point where the radiator mass dominates the system, and the dependence on the other parameters is weak. Thus, as with many space systems, improvements in radiator technology would have a significant impact on the design. This case may also be getting into a regime where neglecting the details of the heat-transfer system and the mass of the input power and power conversion systems is no longer valid. More careful consideration of these systems, which extrapolate significantly beyond terrestrial experience, requires detailed design that is outside the scope of the present paper.

The dependence of the specific power on the magnet shield thickness for the optimized reference cases is shown in Fig. 4. The optimization of the specific power with respect to both the plasma temperature and the ^{3}He-to-D density ratio is shown in Fig. 5 for the mid-term D-^{3}He reference case. The optimum temperature is much higher than that for the plasma power density shown in Fig. 2, because the neutron and bremsstrahlung power fractions decrease with temperature, and reducing them decreases the radiator and refrigerator masses. The dependence of the specific power on the plasma temperature for all three optimized reference cases is shown in Fig. 6.

V. Conclusions

Based on a simple, generic model of the potential performance of a magnetic fusion rocket, the values given by more detailed design studies of 1–10 $kW_{thrust}/kg_{reactor}$ are plausible. The model includes the masses of the systems expected to be the most important contributors to the total mass. Once the physics barriers have been overcome, magnetic fusion propulsion systems appear capable of reaching performance levels of $\sim 10\ \mathrm{kW}_{thrust}/\mathrm{kg}_{reactor}$.

Acknowledgments

Support for this work has been provided by the Grainger Foundation and Lawrence Livermore National Laboratory.

References

[1] S.H. Maslen, "Fusion for Space Propulsion," *IRE Transactions*, Vol. MIL-3, No. 1, 1959, pp. 52–57.

[2] G.W. Englert, "Toward Thermonuclear Rocket Propulsion," *New Scientist*, Vol. 16, No. 307, 1962, pp. 16–18.

[3] N.R. Schulze and J.R. Roth, "The NASA-Lewis Program on Fusion Energy for Space Power and Propulsion, 1958–1978," *Fusion Technology*, Vol. 19, No. 1, 1991, pp. 11–28.

[4] A. Bond, A.R. Martin, R.A. Buckland, T.J. Grant, A.T. Lawton, et al., "Project Daedalus," *Journal of the British Interplanetary Society*, Vol. 31, Supplement, 1978, pp. S1–S192.

[5] C.D. Orth, G. Klein, J. Sercel, N. Hoffman, K. Murray, and F. Chang-Diaz, "The VISTA Spacecraft—Advantages of ICF for Interplanetary Fusion Propulsion Applications," *Twelfth Symposium on Fusion Engineering*, Institute of Electrical and Electronics Engineers, NY, 1987, pp. 1017–1020.

[6] R.W. Bussard, "Fusion as Electric Propulsion," *Journal of Propulsion and Power*, Vol. 6, No. 5, 1990, pp. 567–574.

[7] R.W. Bussard and L.W. Jameson, "Inertial-Electrostatic-Fusion Propulsion Spectrum: Air-Breathing to Interstellar Flight," *Journal of Propulsion and Power*, Vol. 11, No. 2, 1995, pp. 365–372.

[8] C.H. Williams and S.K. Borowski, "An Assessment of Fusion Space Propulsion Concepts and Desired Operating Parameters for Fast Solar System Travel," AIAA Paper 97-3074, July 1997.

[9] S.K. Borowski, "A Comparison of Fusion/Antiproton Propulsion Systems for Interplanetary Travel," AIAA Paper 87-1814, June 1987.

[10] J.F. Santarius, "Lunar ^{3}He, Fusion Propulsion, and Space Development," *Second Conference on Lunar Bases and Space Activities of the 21st Century*, Vol. 1, (Houston, TX, April, 1988), NASA Conf. Pub. 3166, 1992, pp. 75–81.

[11] R. Chapman, G.H. Miley, and W. Kernbichler, "Fusion Space Propulsion with a Field Reversed Configuration," *Fusion Technology*, Vol. 15, No. 2, Part 1, 1989, pp. 1154–1159.

[12] V.E. Haloulakos and R.F. Bourque, "Fusion Propulsion Systems," AIAA Paper 89-2629, July 1989.

[13] E. Teller, A.J. Glass, T.K. Fowler, A. Hasegawa, and J.F. Santarius, "Space Propulsion by Fusion in a Magnetic Dipole," *Fusion Technology*, Vol. 22, No. 1, 1992, pp. 82–97.

[14] S. Carpenter and M. Deveny, "System-Engineering Methods and Design Decisions for the Mirror Fusion Propulsion System (MFPS)," *11th Symposium on Space Nuclear Power and Propulsion*, Part Three, edited by M.S. El Genk and M.D. Hoover, Albuquerque, NM, 1994, pp. 1325–1333.

[15] L.J. Wittenberg, J.F. Santarius, and G.L. Kulcinski, "Lunar Source of ^{3}He for Commercial Fusion Power," *Fusion Technology*, Vol. 10, No. 2, Part 1, 1986, pp. 167–178.

[16] L.J. Wittenberg, E.N. Cameron, G.L. Kulcinski, S.H. Ott, J.F. Santarius, G.I. Sviatoslavsky, I.N. Sviatoslavsky, and H.E. Thompson, "A Review of Helium-3 Resources and Acquisition for Use as Fusion Fuel," *Fusion Technology*, Vol. 21, No. 4, 1992, pp. 2230–2253.

[17] G.H. Miley, "^{3}He Sources for D-^{3}He Fusion Power," *Nuclear Instruments and Methods in Physics Research*, Vol. A271, 1988, pp. 197–202.

[18] J.F. Santarius, "Magnetic Fusion for Space Propulsion," *Fusion Technololgy*, Vol. 21, No. 3, Part 2B, 1992, pp. 1794–1801.

[19] R.F. Post and J.F. Santarius, "Open Confinement Systems and the D-^{3}He Reaction," *Fusion Technology*, Vol. 22, No. 1, 1992, pp. 13–26.

[20] J.F. Santarius, "Magnetic Fusion for Space Propulsion: Capabilities and Issues," *NTSE-92 Nuclear Technologies for Space Exploration*, Vol 2, American Nuclear Society, 1992, pp. 409–418.

[21] J.F. Santarius, G.L. Kulcinski, H. Attaya, M.L. Corradini, L.A. El-Guebaly et al., "SOAR: Space Orbiting Advanced Fusion Power Reactor," *Space Nuclear Power Systems 1987*, Orbit, Malabar, FL, 1988, pp. 167–176.

[22] J.F. Santarius, G.L. Kulcinski, L.A. El-Guebaly, G.A. Emmert, H. Khater et al., "Critical Issues for SOAR: The Space Orbiting Advanced Fusion Power Reactor," *Space Nuclear Power Systems 1988*, Orbit, Malabar, FL, 1989, pp. 161–167.

[23] J.F. Santarius, H.M. Attaya, M.L. Corradini, L.A. El-Guebaly, G.A. Emmert, et al., "Ra: A High Efficiency, D-^{3}He, Tandem Mirror Fusion Reactor," *Twelfth Symposium*

on Fusion Engineering, Institute of Electrical and Electronics Engineers, NY, 1987, pp. 752–755.

[24] J.R. McNally, "Physics of Fusion Fuel Cycles," *Nuclear Fusion/Technology*, Vol. 2, No. 1, 1982, pp. 9–28.

[25] L.M. Hively, "A Simple Computational Form for Maxwellian Reactivities," *Nuclear Technology/Fusion*, Vol. 3, No. 2, 1983, pp. 199–200.

[26] R.A. Gerwin, G.J. Marklin, A.G. Sgro, and A.H. Glasser, "Characterization of Plasma Flow Through Magnetic Nozzles," Air Force Astronautics Laboratory Report AL-TR-89-092, Edwards Air Force Base, CA, February 1990.

[27] E.B. Hooper, "Plasma Detachment from a Magnetic Nozzle," *Journal of Propulsion and Power* Vol. 9, No. 5, 1993, pp. 757–763.

[28] O. Motojima, N. Yanagi, S. Imagawa, K. Takahata, S. Yamada, et al., "Superconducting Magnet Design and Construction of LHD," *Fusion Energy 1996*, Vol. 3, IAEA, Vienna, to be published 1998.

[29] T.R. Strobridge, "Cryogenic Refrigerators–an Updated Survey," National Bureau of Standards Report NBS TN-655, June 1974.

[30] D. Larbalestier, R.D. Blaugher, R.E. Schwall, R.S. Sokolowski, M. Suenaga, and J.O. Willis, "WTEC Panel Report on Power Applications of Superconductivity in Japan and Europe," World Technology Evaluation Center Report PB98-103161, National Technical Information Service, VA, September 1997.

[31] L.A. El-Guebaly, “Magnet Shielding Analysis for SOAR—A Space Reactor,” *Space Nuclear Power Systems 1987*, Orbit, Malabar, FL, 1988, pp. 147–153.

[32] E. Stuhlinger, *Ion Propulsion for Space Flight* (McGraw-Hill, NY, 1964).

[33] K.A. Ehricke, *Space Flight, Vol II: Dynamics* (Van Nostrand, Princeton, 1962).

List of Tables

Table 1: Some recent conceptual designs studies of magnetic fusion reactors for space propulsion

First Author	Year	Configuration	Specific Power (kW/kg)
Borowski [9]	1987	Spherical Torus	5.75
Borowski [9]	1987	Spheromak	10.5
Santarius [21]	1988	Tandem Mirror	1.2
Chapman [11]	1989	Field-Reversed Configuration	–
Haloulakis [12]	1989	Colliding Spheromaks	–
Bussard [6]	1990	Riggatron Tokamak	3.9
Teller [13]	1992	Dipole	1.0
Deveny [14]	1994	Tandem Mirror	4.0

Table 2: Engineering parameter default assumptions

Parameter	Mid-term	Long-term
Surface heat flux limit, MW/m^2	5	10
Neutron wall load limit, MW/m^2	20	20
Magnet winding pack average current density, MA/m^2	50	250
Magnet stored energy per unit mass, kJ/kg	50	200
Magnet winding pack average density, Mg/m^3	6	6
He-refrigerator mass per heat pumped, kg/kW	1000	1000
Radiator: power rejected per unit mass, kW/kg	5	5
Shield density, Mg/m^3	1	1
Shield thickness for 10-fold magnet heating reduction, m	0.31	0.31
Shield-magnet gap, m	0.1	0.1
Halo thickness, m	0.1	0.1
Efficiency of transforming transport power to thrust	0.8	0.8

Table 3: Reference parameters for three generic fusion rocket cases

Parameter	Mid-term D-T	Mid-term D-^{3}He	Long-term D-^{3}He
β	0.6	0.6	0.9
Deuterium density, m^{-3}	5.7×10^{20}	3.7×10^{20}	6.4×10^{20}
T- or ^{3}He-to-D density ratio	1	0.68	0.66
Plasma temperature, keV	17	100	128
Plasma length, m	71	5.1	3.7
Plasma radius, m	0.25	1.12	0.67
Shield thickness, m	0.42	0.19	0.29
Magnetic field, T	5	10	12
Magnet stored energy, GJ	1.7	1.5	0.88
Thrust power, MW	600	600	600
Fusion power, MW	3960	992	968
Bremsstrahlung power, MW	45	196	176
Neutron power, MW	3166	46	42
Neutron wall load, MW/m^2	20	1.12	2.39
Surface heat flux, MW/m^2	0.28	5	10
Magnet mass, Mg	187	46	6.1
Radiator mass, Mg	642	48	44
Refrigerator mass, Mg	64	9.4	3.6
Shield mass, Mg	106	8.2	6.1
Total mass, Mg	999	112	59
Specific power, kW/kg	0.60	5.3	10.1

List of Figures

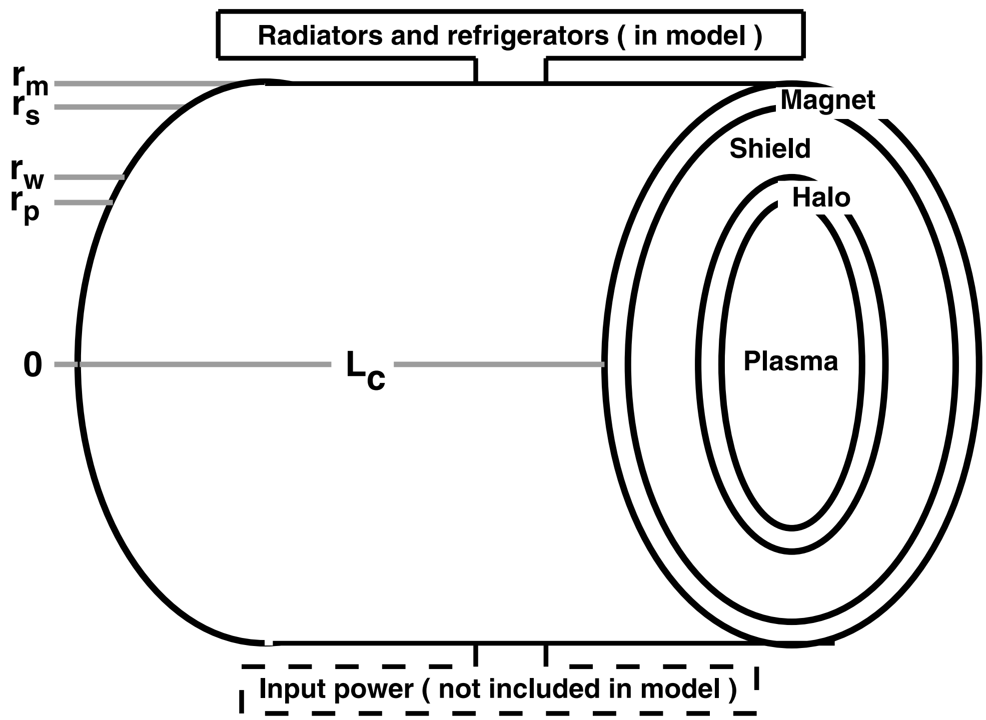

Figure 1: Generic fusion rocket geometry.

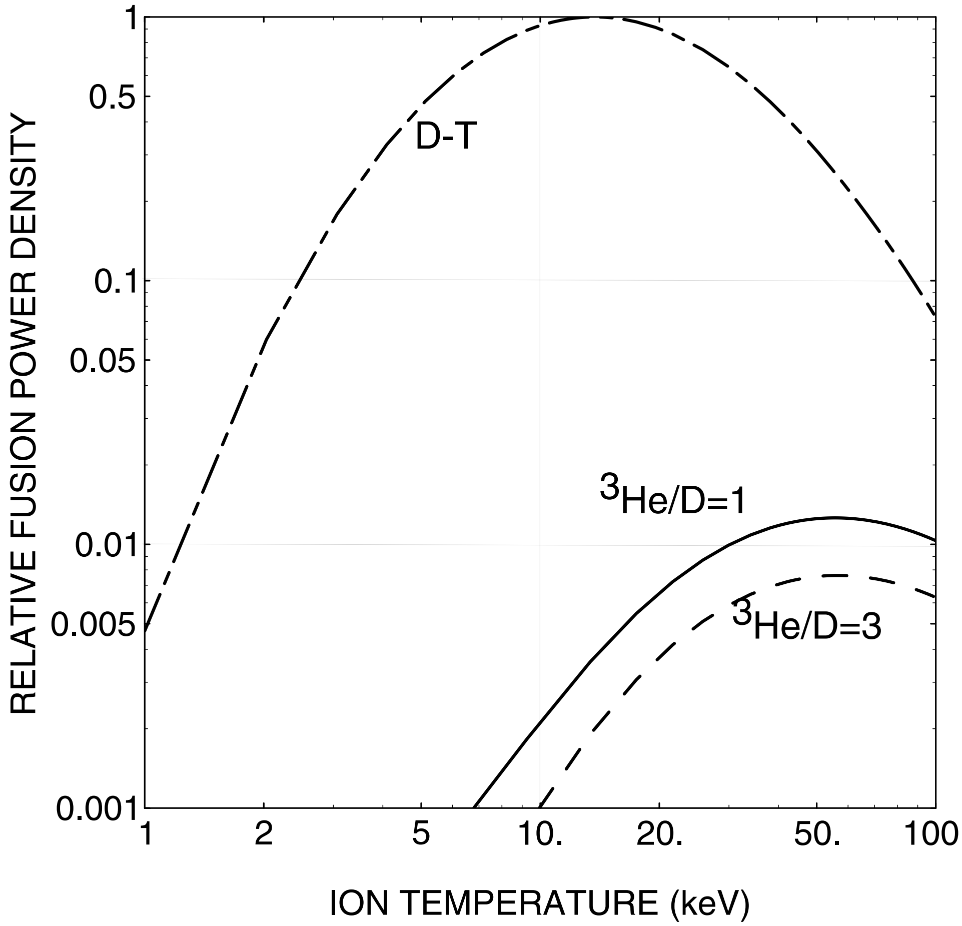

Figure 2: Local fusion power density in the plasma for D-T and D-^{3}He fusion fuels, with two values of the ^{3}He-to-D density ratio shown.

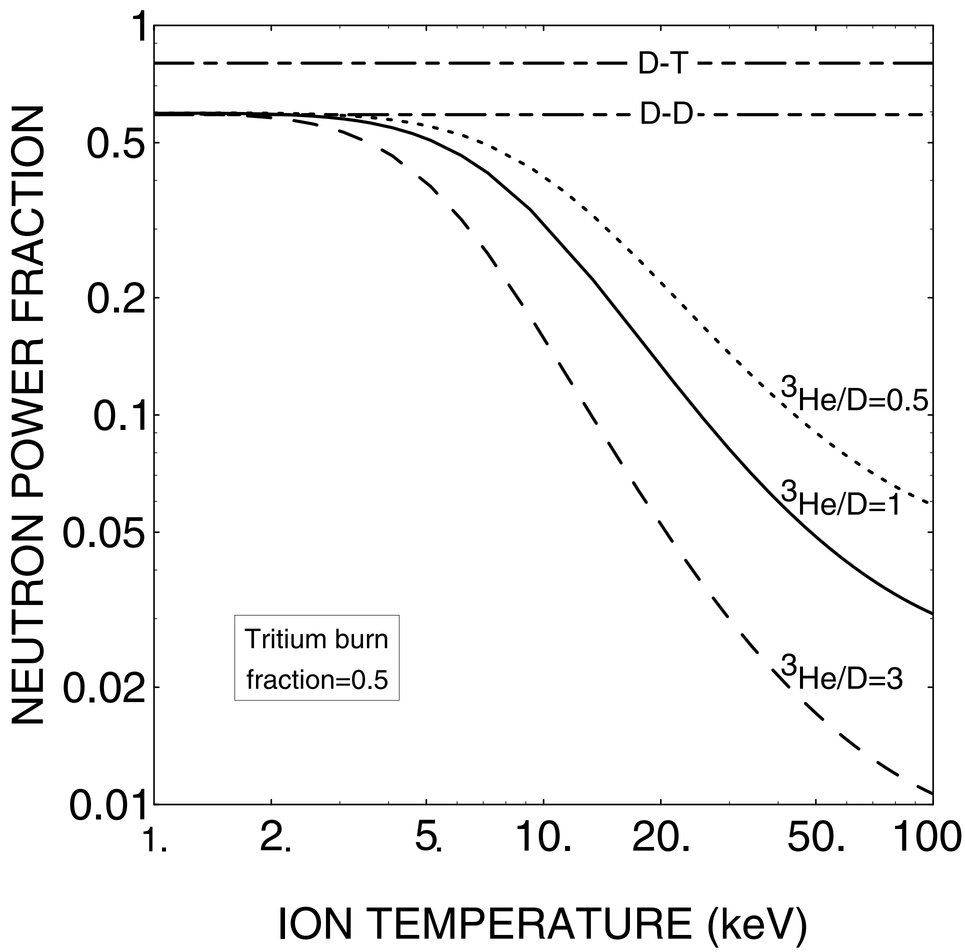

Figure 3: Ratio of neutron power to fusion power for the D-T, D-D, and D-^{3}He fusion fuel cycles, with three values of the ^{3}He-to-D density ratio shown.

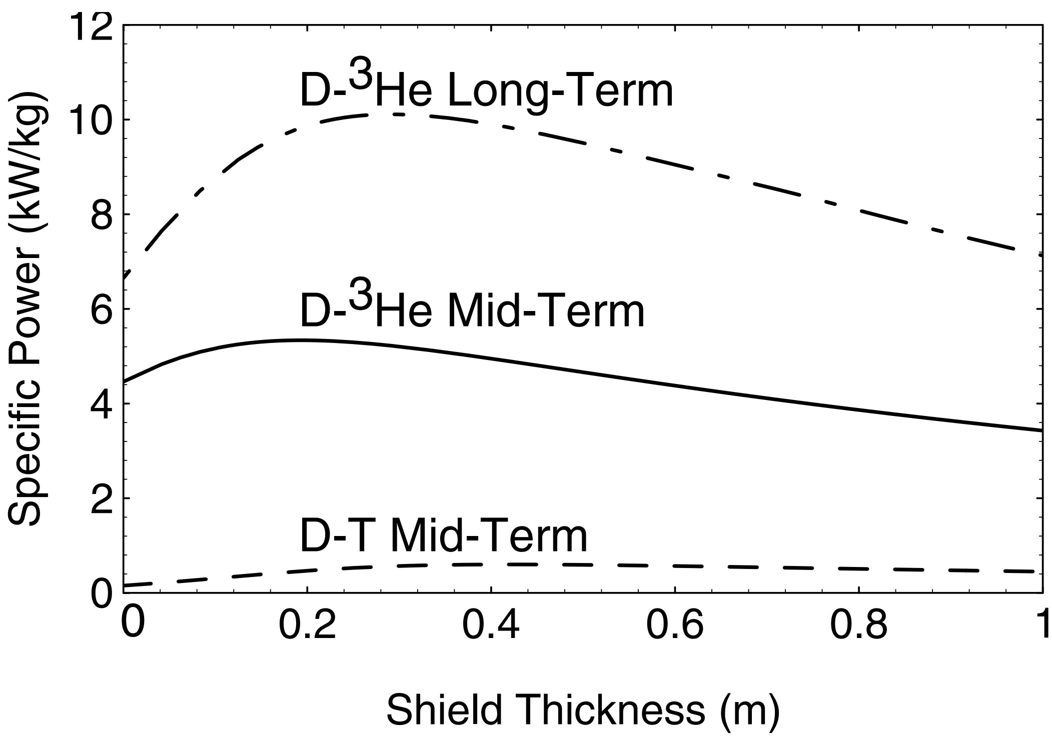

Figure 4: Dependence of specific power on shield thickness for the generic fusion rocket reference cases.

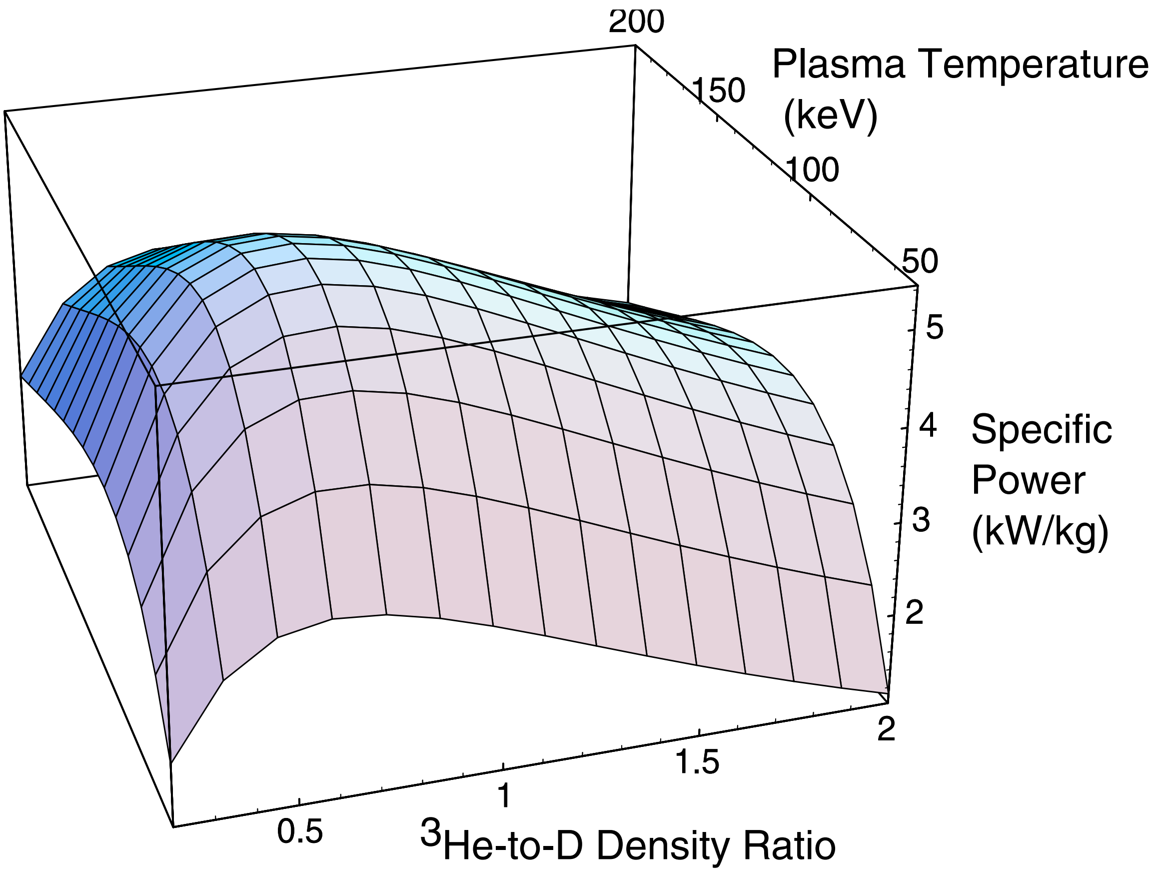

Figure 5: Dependence of specific power on plasma temperature and the ^{3}He-to-D density ratio for the mid-term D-^{3}He fusion rocket reference case.

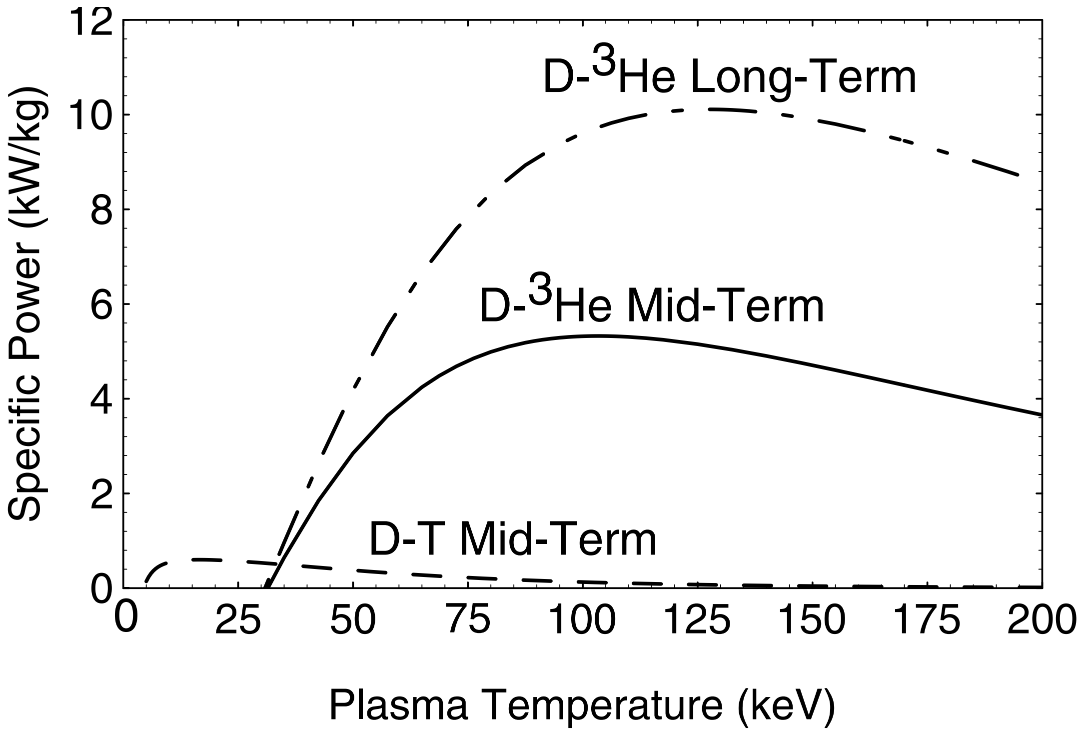

Figure 6: Dependence of specific power on plasma temperature for the generic fusion rocket reference cases.